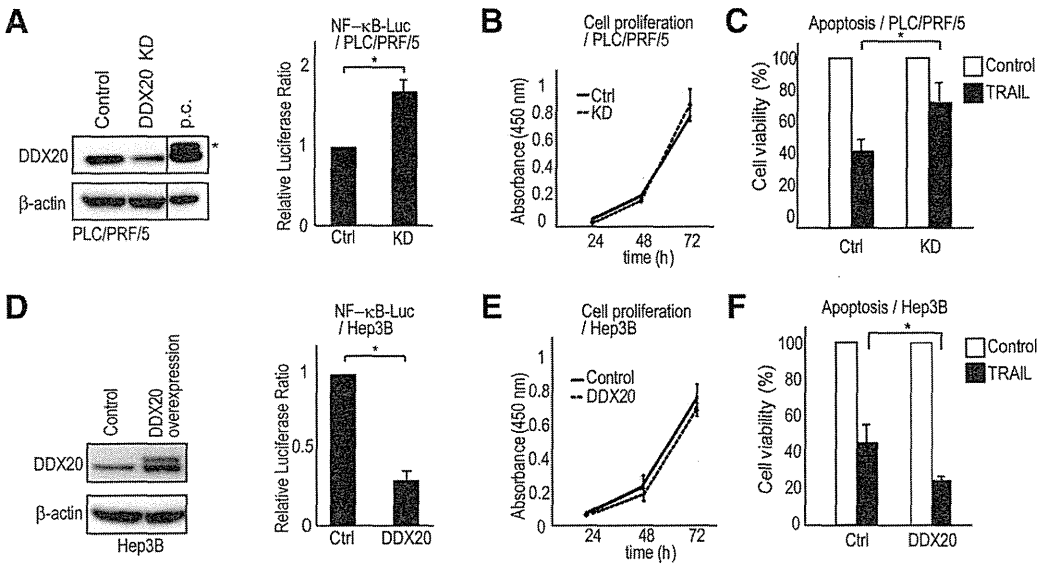

Fig. 2. Modulation of downstream events of the nuclear factor-κB pathway by DDX20. (A) Left: Establishment of stable DDX20-knockdown (DDX20 KD) PLC/PRF/5 cells. *Positive control (p.c.). Right: DDX20 deficiency enhances TNF-α–induced NF-κB activity. NF-κB reporter plasmids were transiently transfected into control (Ctrl) or DDX20-knockdown (KD) PLC/PRF/5 cells. The cells were then treated with TNF-α (5 ng/mL) or vehicle for 6 hours. *$P < 0.05$. Data are presented as the mean ± SD of three independent determinations. (B) Cell proliferation rates were comparable for control (Ctrl) and DDX20-knockdown (KD) PLC/PRF/5 cells. Data are presented as the mean ± SD of three determinations. (C) DDX20 deficiency reduces TRAIL-induced apoptotic cell death. Control (Ctrl) and DDX20-knockdown (KD) PLC/PRF/5 cells were incubated with 25 ng/mL TRAIL. Data represent cell viability after TRAIL stimulation (gray bars) relative to the number of vehicle-treated cells (white bars). *$P < 0.05$. Data are presented as the mean ± SD of triplicate determinations. (D) Left: Establishment of stable DDX20-overexpressing cells. Hep3B cells were infected with control or FLAG-tagged DDX20-overexpressing lentiviruses and selected on puromycin. Western blot analysis confirmed increased expression of DDX20 protein. Right: DDX20 overexpression suppresses TNF-α–induced NF-κB activity. NF-κB reporter plasmids were transiently transfected into Hep3B control (Ctrl) and DDX20-overexpressing (DDX20) cells treated with TNF-α for 6 hours. Data are presented as the mean ± SD of three independent determinations. *$P < 0.05$. (E) Proliferation of control (Ctrl) and DDX20-overexpressing (DDX20) Hep3B cells was measured as described in (B). (F) DDX20 overexpression reduces TRAIL-induced apoptotic cell death. Data for control (Ctrl) and DDX20-overexpressing (DDX20) Hep3B cells are shown. *$P < 0.05$.

Table 2. Increased Expression of NF-κB–Related Genes in DDX20-Knockdown HepG2 Cells Compared with Wild-Type Cells

RefSeq ID	Symbol	Description	Ratio	Representative Gene Function
NM_000639	FASLG	Fas ligand	3.5	NF-κB target, apoptosis
NM_052813	C9orf151	CARD9	2.5	NF-κB cascade, NF-κB target
NM_014959	CARD8	Tumor up-regulated CARD-containing antagonist of CASP9 (TUCAN)	2.2	NF-κB target
NM_131917	FAF1	FAS-associated factor 1 (hFAF1)	1.9	Cytoplasmic sequestering of NF-κB, NF-κB target
NM_020644	TMEM9B	Transmembrane protein 9B precursor	1.9	Positive regulation of NF-κB transcription factor activity
NM_017544	NKRF	ITBA4 protein	1.9	Negative regulation of transcription
NM_006247	PPP5C	Protein phosphatase T	1.8	Positive regulation of NF-κB cascade
NM_020345	NKIRAS1	KappaB-Ras1	1.8	NF-κB cascade
NM_001569	IRAK1	IRAK-1	1.7	Positive regulation of NF-κB transcription factor activity
NM_177951	PPM1A	Protein phosphatase 1A	1.7	Positive regulation of NF-κB cascade
NM_018098	ECT2	Epithelial cell-transforming sequence 2 oncogene	1.6	Positive regulation of NF-κB cascade
NM_002305	LGALS1	Galectin-1 (putative MAPK-activating protein MP12)	1.6	Positive regulation of NF-κB cascade
NM_015093	TAB2	TAK1-binding protein 2	1.6	Positive regulation of NF-κB cascade
NM_004180	TANK	TRAF-interacting protein	1.5	NF-κB cascade
NM_014976	PDCD11	Programmed cell death protein 11	1.5	rRNA processing
NM_015336	ZDHHC17	Putative NF-κB-activating protein 205	1.5	Positive regulation of NF-κB cascade
NM_002503	NFKBIB	IKB-β	1.5	Cytoplasmic sequestering of NF-κB
NM_138330	ZNF675	Zinc finger protein 675	1.5	Negative regulation of NF-κB transcription factor activity

The genes were identified as NF-κB–related based on the Gene Ontology and the GeneCodis Databases.

Table 3. Decreased Expression Levels of MT Genes in DDX20 Knockdown HepG2 Cells Compared with Wild-Type Cells

Symbol	Description	Ratio
MT1E	Metallothionein-1E	**0.12**
MT1F	Metallothionein-1F	**0.36**
MT1H	Metallothionein-1H	**0.16**
MT1G	Metallothionein-1G	**0.06**
MT1M	Metallothionein-1M	**0.24**
MT1X	Metallothionein-1X	**0.27**
MT2A	Metallothionein-2	**0.28**
MT3	Metallothionein-3	0.84
MTL5	Metallothionein-like 5 (Tesmin)	1.12

Numbers in boldface type indicate values <0.5.

expression levels of a group of metallothioneins (MTs), such as MT1E, MT1F, MT1G, MT1M, MT1X, and MT2A, were all significantly decreased when DDX20 was deficient (Table 3). The decreased expression of MTs in DDX20-knockdown HepG2 and PLC/PRF/5 cells was confirmed via quantitative RT-PCR (Fig. 3a and Supporting Fig. 3). Expression of MT-3, which was not altered in the microarray analysis, was similarly unaltered in quantitative RT-PCR analysis. Notably, it was already known that MTs are frequently silenced in human primary liver cancers.[34-36] In addition, MT knockout mice have enhanced NF-κB activity, likely due to reactive oxygen species, and these mice are more prone to hepatocarcinogenesis.[37] These results suggest that DDX20 deficiency enhances NF-κB activity by decreasing the expression of MTs, which could facilitate the development of liver cancer.

MiRNA-140 Directly Targets Dnmt1. Because MT expression is regulated principally by CpG island methylation in their promoter regions,[38,39] we examined the quantitative methylation status of MT promoters in DDX20-knockdown cells. The CpG islands of the MT1E, MT1G, MT1M, MT1X, and MT2A promoters, and the CpG shores of the MT1F promoters, were significantly more highly methylated under DDX20-deficient conditions, as determined by the comprehensive Illumina Quantitative Methylation BeadChip method (Table 4, Supporting Table 2, and GSE 37633). A crucial step in DNA methylation involves DNA methyltransferase (Dnmt), which catalyzes the methylation of CpG dinucleotides in genomic DNA.[40] The methylation status of MT promoters is mediated specifically by Dnmt1.[41] Because Dnmt1 contains a predicted miRNA-140-3p target site in its 3′ UTR, with a perfect match to its seed sequences (Fig. 3B), and because the effects of miRNA-140-3p activity were impaired in DDX20-knockdown cells,[23] it was hypothesized that whereas miRNA-140 normally targets and suppresses Dnmt1 protein expression, miRNA-140-3p dysfunction due to DDX20 deficiency results in enhanced Dnmt1 expression, leading to hypermethylation of MT promoters. Consistent with this hypothesis, Dnmt1 expression was increased significantly in DDX20-knockdown cells (Fig. 3C). miRNA-140 precursor overexpression suppressed activity of the Dnmt1 3′ UTR reporter construct, the effect of which was lost when two mutations were introduced into its seed sequences (Fig. 3D). MiRNA-140 precursor overexpression suppressed Dnmt1 protein expression (Fig. 3E). These results indicate that miRNA-140 directly targets Dnmt1 and suppresses its expression in the normal state. Consistently, decreased DDX20, increased Dnmt1, and decreased MT expression were detected together in human clinical HCC samples, as determined via immunohistochemistry (Fig. 3F). By contrast, miRNA-140 precursor-overexpressing Huh7 cells showed increased expression of MTs and reduced NF-κB activity *in vitro* (Supporting Fig. 4A,B). Moreover, the increase in the number of spheres formed from PLC/PRF/5 cells due to DDX20 knockdown was antagonized by treatment with an NF-κB inhibitor or a demethylating agent (Supporting Fig. 5). Taken together, these results suggest that the up-regulated Dnmt1 protein expression caused by functional impairment of miRNA-140-3p due to DDX20 deficiency results in decreased expression of MTs *via* enhanced methylation at the CpG sites in their promoters. This may lead to enhanced NF-κB activity and cellular transformation at least *in vitro*.

MiRNA-140 Is a Liver Tumor Suppressor. To further examine the biological consequences of functional impairment of miRNA-140 due to DDX20 deficiency, we determined the phenotypes of miRNA-140 knockout (miRNA-140$^{-/-}$) mice (Fig. 4A). Similar to the *in vitro* DDX20 knockdown results, Dnmt1 expression was increased and MT levels decreased in the liver tissue of these mice (Fig. 4B). NF-κB–DNA binding activity was enhanced in the livers of miRNA-140$^{-/-}$ mice after tail-vein injection of TNF-α, a crucial cytokine that induces NF-κB activity and hepatocarcinogenesis (Fig. 4C). As was found in MT knockout mice, phosphorylation of p65 at serine 276, which is critical for p65 activation, was significantly increased in the livers of miRNA-140$^{-/-}$ mice after DEN exposure, which induces NF-κB activation and liver tumors[37] (Fig. 4D). Notably, the size and number of liver tumors that developed 8 months after DEN exposure were markedly elevated in miRNA-140$^{-/-}$ mice compared with control mice (Fig. 4E,F). These results indicate that miRNA-140$^{-/-}$ mice are indeed

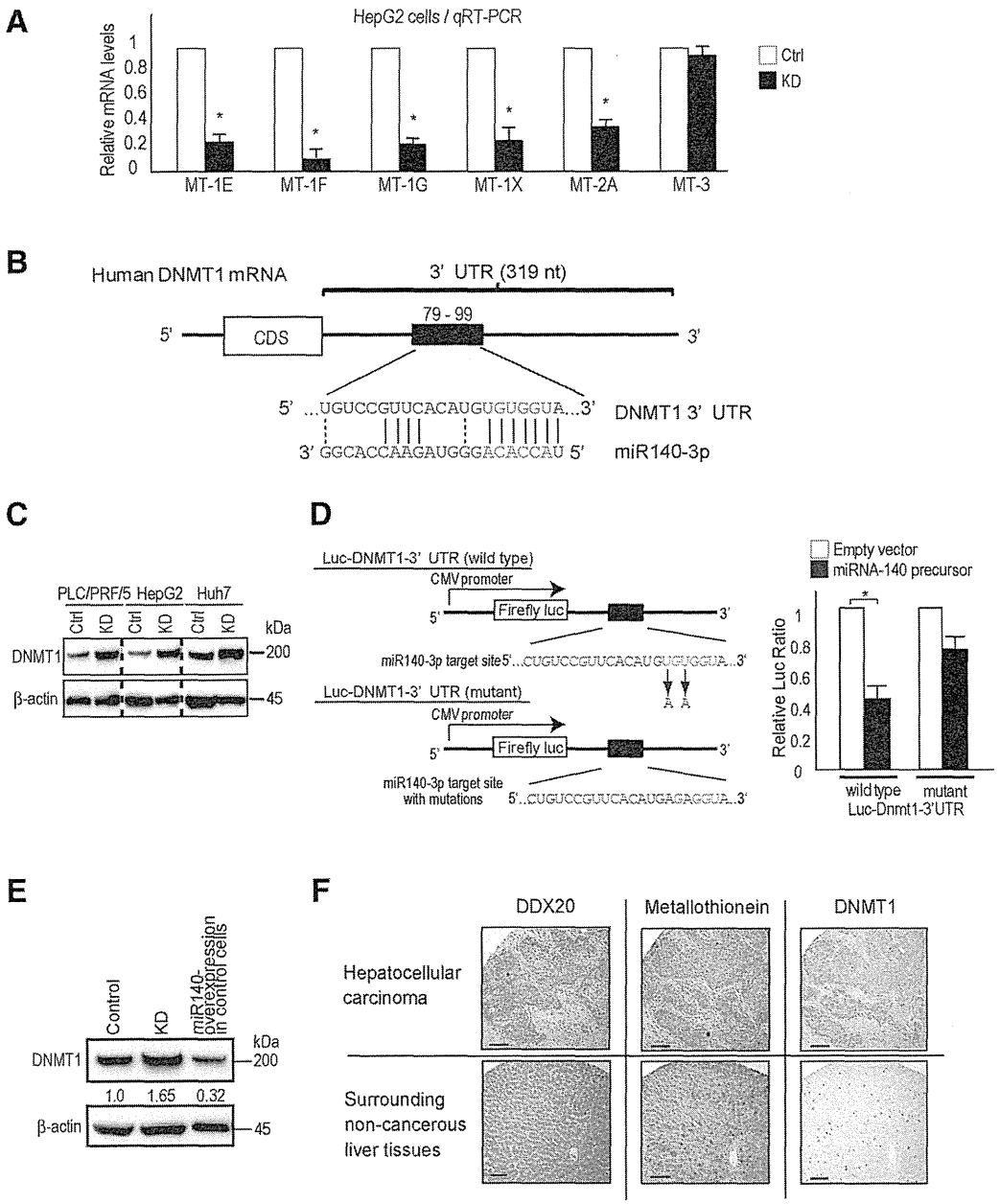

Fig. 3. Targeting of Dnmt1 by miRNA-140-3p and reduced MT expression. (A) The expression levels of MTs were determined using quantitative reverse-transcriptase polymerase chain reaction. The relative expression ratios of the MTs in control (white bars) and DDX20-knockdown (black bars) HepG2 cells were calculated by normalizing control cell values to 1.0. The data represent the mean ± SD of three independent determinations. *$P < 0.05$. (B) Putative miRNA-140-3p target sites in the 3′ UTR of human Dnmt1. Seed sequences are indicated in red. (C) Dnmt1 expression was increased in DDX20-knockdown cells. Ctrl, control cells; KD, DDX20-knockdown cells. (D) Left: Schematic diagrams of wild-type (upper) and mutant (lower) luciferase reporter constructs (Luc-Dnmt1-3′ UTRs) carrying the Dnmt1 3′ UTR region harboring the putative miRNA-140-3p target site. The mutant seed sequence contained two nucleotide substitutions. Right: The Dnmt1 3′ UTR is targeted directly by miRNA-140-3p. Cells were cotransfected with Luc-Dnmt1-3′ UTR (wild-type or mutant) plus either an empty vector (white bars) or a plasmid expressing the miRNA-140 precursor (black bars). Data are the mean ± SD of three independent determinations. (E) Overexpression of miRNA-140 reduces Dnmt1 expression in control cells. Values between the panels indicate Dnmt1 protein levels normalized to those of β-actin. KD, DDX20 knockdown cells. (F) Representative histochemical images showing expression of DDX20, Dnmt1, and MT proteins in HCC (upper three panels) and surrounding tissue (lower panels). Compared with adjacent noncancerous liver tissue, HCCs exhibited decreased DDX20 and MT expression and increased Dnmt1 expression. Note that adjacent sections were stained for each protein. Scale bar, 50 μm.

Table 4. Methylation Levels in CpG Islands of the MT Genes in DDX20-Knockdown HepG2 Cells Compared with Control Cells

Symbol	CpG Island Methylation Ratio	Target ID
MT1E	**1.14**	cg00178359
	1.29	cg06463589
	3.65	cg02512505
	1.02	cg15134649
MT1G	**2.14**	cg16452857
	1.03	cg27367960
	1.00	cg03566142
	0.99	cg07791866
MT1M	**1.16**	cg02132560
	0.98	cg02160530
	1.03	cg04994964
MT1X	**1.24**	cg05596720
	1.05	cg26802333
	1.06	cg09147880
	1.01	cg08872713
MT2A	**2.06**	cg07395075
	0.94	cg20430434

Values were determined using the quantitative Illumina Human Methylation BeadsChip. Boldface values indicate increased methylation levels in DDX20 knockdown cells.

more prone to liver cancer development and suggest that miRNA-140 acts as a liver tumor suppressor, probably by suppressing NF-κB activity, although we cannot completely exclude other molecular mechanisms. Nonetheless, these results also suggest that the impairment of miRNA-140 function due to DDX20 deficiency may lead to hepatocarcinogenesis in humans, as we have observed in miRNA-140$^{-/-}$ mice (Supporting Figs. 6 and 7).

Discussion

Here, we report that miRNA-140$^{-/-}$ mice have increased NF-κB activity and are more prone to HCC development. In addition, we show that DDX20, an miRNP component, is frequently decreased in human HCC tissues. Because DDX20 deficiency preferentially causes impaired miRNA-140 function,[23] the functional impairment of miRNA-140 may result in phenotypes similar to those of miRNA-140$^{-/-}$ mice and may lead to hepatocarcinogenesis. In support of the hypothesis that DDX20 dysfunction is involved in hepatocarcinogenesis, DDX20 is located at 1p21.1-p13.2, a frequently deleted chromosomal region in human HCC,[27] and DDX20 was recently identified as a possible liver tumor suppressor in a functional screen in mice.[27] Although the possibility that intracellular signaling pathways other than miRNA-140 may also be involved in the biological consequences of DDX20 deficiency cannot be denied, we believe that functional impairment of miRNA-140 plays a major role in the phenotypes induced by DDX20 deficiency, based on the phenotypic similarities.

Changes in miRNA expression levels have been reported in various tumors.[7,12,42] However, in this study, we found that reduced expression of an miRNA machinery component might lead to carcinogenesis, at least in part, through functional impairment of miRNAs. Recent studies have shown that components of the RNA interference machinery are associated with the outcome of ovarian cancer patients,[43] and that single-nucleotide polymorphisms in miRNA machinery genes can be used as diagnostic risk markers.[44,45] Therefore, the impairment of miRNA function caused by deregulated miRNA machinery components may also be involved in carcinogenesis.

Our study identified Dnmt1 as a critical target of miRNA-140. The decreased MT expression due to the CpG promoter methylation induced by Dnmt1 resulted in enhanced NF-κB activity. This finding was consistent with the results obtained using MT gene knockout mice, in which enhanced NF-κB activation promoted hepatocarcinogenesis.[37] The decrease in MT expression that results from increased Dnmt1 expression caused by functional impairment of miRNA-140, together with increased NF-κB activation and hepatocarcinogenesis in MT knockout mice,[37] supports the concept that the DDX20/miRNA-140/Dnmt1/MT/NF-κB pathway may play a crucial role in hepatocarcinogenesis. However, we cannot fully exclude the possibility that other intracellular signaling pathways are also involved in the induction of hepatocarcinogenesis by miRNA-140 or DDX20 deficiency, because the precise role of NF-κB in hepatocarcinogenesis has not been clearly defined,[8] although constitutive activation of NF-κB signaling has been frequently detected in human HCCs.[46] The mechanisms by which DDX20 expression is initially decreased and the reason its locus is frequently deleted in HCC remain to be elucidated. However, because DDX20 expression is also regulated by methylation of its CpG promoter,[47] once this pathway is deregulated, decreased DDX20 expression could be maintained by a positive feedback mechanism, even without deletion of its locus.[27]

In conclusion, this study shows that miRNA-140 acts as a liver tumor suppressor. We show that DDX20, an miRNP component, is frequently decreased in human HCC, which may induce hepatocarcinogenesis via impairment of miRNA-140 function. These results suggest the importance of investigations of not only aberrant miRNA expression levels,[12,14,17,48] but also deregulation of miRNP

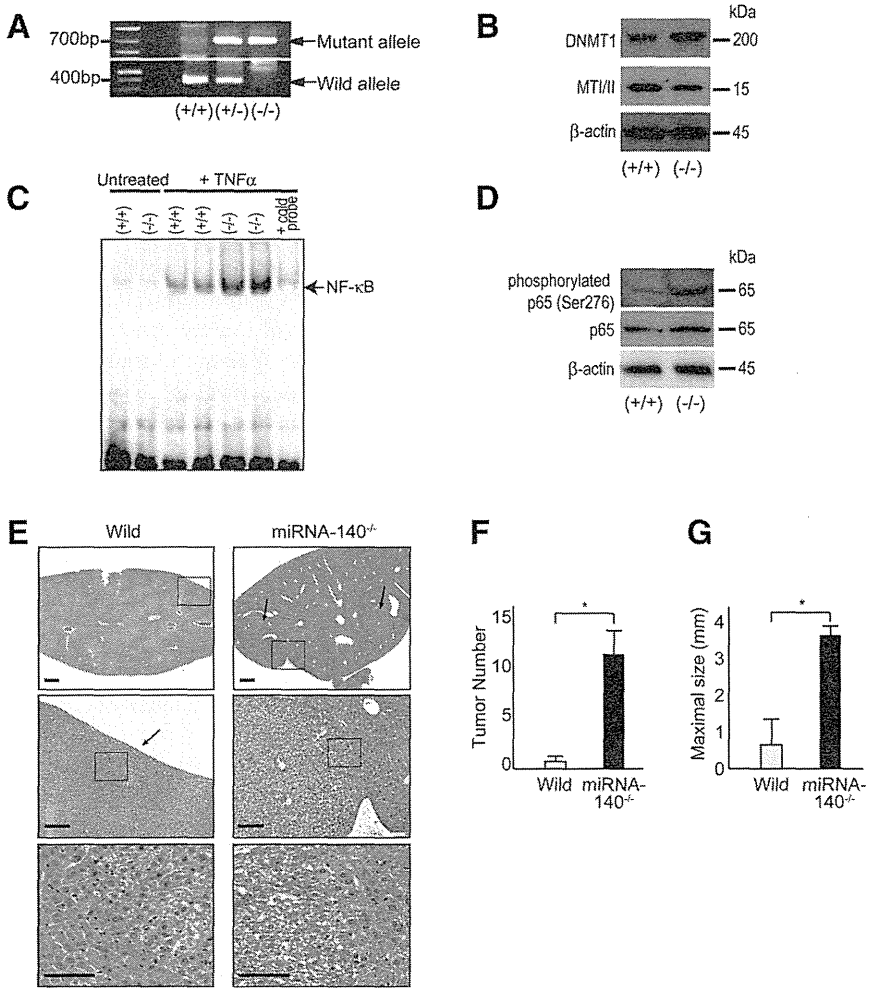

Fig. 4. miRNA-140$^{-/-}$ mice are prone to hepatocarcinogenesis. (A) Representative genotyping of mice with wild-type or mutant alleles. PCR genotyping was performed for miRNA-140 wild-type (419 bp; Wild) and knockout (734 bp; Mutant) alleles. (+/+), wild-type; (+/−), heterozygous; (−/−), knockout. (B) Increased Dnmt1 expression and decreased MTI/II expression in the liver tissues of miRNA-140$^{-/-}$ mice compared with wild-type mice. Western blotting was performed using antibodies against the indicated proteins. (+/+), wild-type; (−/−), miRNA-140$^{-/-}$. The image shown is representative of four independent experiments. (C) NF-κB-DNA binding was assessed via gel-shift assay using equal amounts of liver nuclear extracts from untreated and TNF-α-injected wild-type and miRNA-140$^{-/-}$ mice. (+/+), wild-type; (−/−), miRNA-140$^{-/-}$. Cold probe was added to TNF-α-injected knockout mouse nuclear extract to test assay specificity. A result representative of four independent experiments is shown. (D) Western blotting for phosphorylated p65 expression in the liver at 32 weeks after DEN treatment in miRNA-140$^{-/-}$ mice compared with wild-type mice. A result representative of four independent experiments is shown. (E) Representative histological images of mouse liver at 32 weeks after DEN treatment. Arrows indicate tumors. Higher-magnification images of the highlighted areas in the upper panels are shown in the lower panels. Scale bar, 500 μm. (F) The number (left panel) and size (right panel) of tumors (five random sections per mouse treated with DEN) are presented as the mean ± SD (wild-type mice, n = 8; miRNA-140$^{-/-}$ mice, n = 8). *$P < 0.05$.

components,[22] with subsequent impairment of miRNA function as molecular pathways and possible therapeutic targets for carcinogenesis and other diseases.

References

1. Parkin D, Bray F, Ferlay J, Pisani P. Global cancer statistics, 2002. CA Cancer J Clin 2005;55:74-108.
2. Block T, Mehta A, Fimmel C, Jordan R. Molecular viral oncology of hepatocellular carcinoma. Oncogene 2003;22:5093-5107.
3. Karin M. Nuclear factor-kappaB in cancer development and progression. Nature 2006;441:431-436.
4. Luedde T, Schwabe RF. NF-κB in the liver—linking injury, fibrosis and hepatocellular carcinoma. Nat Rev Gastroenterol Hepatol 2011;8:108-118.
5. Pikarsky E, Porat R, Stein I, Abramovitch R, Amit S, Kasem S, et al. NF-kappaB functions as a tumour promoter in inflammation-associated cancer. Nature 2004;431:461-466.
6. Liu P, Kimmoun E, Legrand A, Sauvanet A, Degott C, Lardeux B, et al. Activation of NF-kappa B, AP-1 and STAT transcription factors is a frequent and early event in human hepatocellular carcinomas. J Hepatol 2002;37:63-71.

7. Ji J, Shi J, Budhu A, Yu Z, Forgues M, Roessler S, et al. MicroRNA expression, survival, and response to interferon in liver cancer. N Engl J Med 2009;361:1437-1447.
8. Feng GS. Conflicting roles of molecules in hepatocarcinogenesis: paradigm or paradox. Cancer Cell 2012;21:150-154.
9. Bartel DP. MicroRNAs: target recognition and regulatory functions. Cell 2009;136:215-233.
10. Otsuka M, Jing Q, Georgel P, New L, Chen J, Mols J, et al. Hypersusceptibility to vesicular stomatitis virus infection in Dicer1-deficient mice is due to impaired miR24 and miR93 expression. Immunity 2007;27:123-134.
11. Otsuka M, Zheng M, Hayashi M, Lee JD, Yoshino O, Lin S, et al. Impaired microRNA processing causes corpus luteum insufficiency and infertility in mice. J Clin Invest 2008;118:1944-1954.
12. Kojima K, Takata A, Vadnais C, Otsuka M, Yoshikawa T, Akanuma M, et al. MicroRNA122 is a key regulator of α-fetoprotein expression and influences the aggressiveness of hepatocellular carcinoma. Nat Commun 2011;2:338.
13. Chang T-C, Yu D, Lee Y-S, Wentzel EA, Arking DE, West KM, et al. Widespread microRNA repression by Myc contributes to tumorigenesis. Nat Genet 2008;40:43-50.
14. Lu J, Getz G, Miska EA, Alvarez-Saavedra E, Lamb J, Peck D, et al. MicroRNA expression profiles classify human cancers. Nature 2005; 435:834-838.
15. Calin GA, Croce CM. MicroRNA signatures in human cancers. Nat Rev Cancer 2006;6:857-866.
16. Gaur A, Jewell DA, Liang Y, Ridzon D, Moore JH, Chen C, et al. Characterization of microRNA expression levels and their biological correlates in human cancer cell lines. Cancer Res 2007;67:2456-2468.
17. Kumar MS, Lu J, Mercer KL, Golub TR, Jacks T. Impaired microRNA processing enhances cellular transformation and tumorigenesis. Nat Genet 2007;39:673-677.
18. Lambertz I, Nittner D, Mestdagh P, Denecker G, Vandesompele J, Dyer MA, et al. Monoallelic but not biallelic loss of Dicer1 promotes tumorigenesis in vivo. Cell Death Differ 2010;17:633-641.
19. Otsuka M, Takata A, Yoshikawa T, Kojima K, Kishikawa T, Shibata C, et al. Receptor for activated protein kinase C: requirement for efficient microRNA function and reduced expression in hepatocellular carcinoma. PLoS One 2011;6:e24359.
20. Lujambio A, Esteller M. CpG island hypermethylation of tumor suppressor microRNAs in human cancer. Cell Cycle 2007;6:1455-1459.
21. Thomson J, Newman M, Parker J, Morin-Kensicki E, Wright T, Hammond S. Extensive post-transcriptional regulation of microRNAs and its implications for cancer. Genes Dev 2006;20:2202-2207.
22. Melo SA, Ropero S, Moutinho C, Aaltonen LA, Yamamoto H, Calin GA, et al. A TARBP2 mutation in human cancer impairs microRNA processing and DICER1 function. Nat Genet 2009;41:365-370.
23. Takata A, Otsuka M, Yoshikawa T, Kishikawa T, Kudo Y, Goto T, et al. A miRNA machinery component DDX20 controls NF-κB via microRNA-140 function. Biochem Biophys Res Commun 2012;13:564-569.
24. Miyaki S, Sato T, Inoue A, Otsuki S, Ito Y, Yokoyama S, et al. MicroRNA-140 plays dual roles in both cartilage development and homeostasis. Genes Dev 2010;24:1173-1185.
25. Garzon R, Heaphy CE, Havelange V, Fabbri M, Volinia S, Tsao T, et al. MicroRNA 29b functions in acute myeloid leukemia. Blood 2009;114:5331-5341.
26. Mourelatos Z, Dostie J, Paushkin S, Sharma A, Charroux B, Abel L, et al. miRNPs: a novel class of ribonucleoproteins containing numerous microRNAs. Genes Dev 2002;16:720-728.
27. Zender L, Xue W, Zuber J, Semighini C, Krasnitz A, Ma B, et al. An oncogenomics-based in vivo RNAi screen identifies tumor suppressors in liver cancer. Cell 2008;135:852-864.
28. Mouillet J, Yan X, Ou Q, Jin L, Muglia L, Crawford P, et al. DEAD-box protein-103 (DP103, Ddx20) is essential for early embryonic development and modulates ovarian morphology and function. Endocrinology 2008;149:2168-2175.
29. Voss M, Hille A, Barth S, Spurk A, Hennrich F, Holzer D, et al. Functional cooperation of Epstein-Barr virus nuclear antigen 2 and the survival motor neuron protein in transactivation of the viral LMP1 promoter. J Virol 2001;75:11781-11790.
30. Charroux B, Pellizzoni L, Perkinson R, Shevchenko A, Mann M, Dreyfuss G. Gemin3: a novel DEAD box protein that interacts with SMN, the spinal muscular atrophy gene product, and is a component of gems. J Cell Biol 1999;147:1181-1194.
31. Hutvágner G, Zamore P. A microRNA in a multiple-turnover RNAi enzyme complex. Science 2002;297:2056-2060.
32. Takata A, Otsuka M, Kojima K, Yoshikawa T, Kishikawa T, Yoshida H, et al. MicroRNA-22 and microRNA-140 suppress NF-κB activity by regulating the expression of NF-κB coactivators. Biochem Biophys Res Commun 2011;411:826-831.
33. Hu W, Johnson H, Shu H. Tumor necrosis factor-related apoptosis-inducing ligand receptors signal NF-kappaB and JNK activation and apoptosis through distinct pathways. J Biol Chem 1999;274: 30603-30610.
34. Cherian MG, Jayasurya A, Bay BH. Metallothioneins in human tumors and potential roles in carcinogenesis. Mutat Res 2003;533:201-209.
35. Huang GW, Yang LY. Metallothionein expression in hepatocellular carcinoma. World J Gastroenterol 2002;8:650-653.
36. Datta J, Majumder S, Kutay H, Motiwala T, Frankel W, Costa R, et al. Metallothionein expression is suppressed in primary human hepatocellular carcinomas and is mediated through inactivation of CCAAT/enhancer binding protein alpha by phosphatidylinositol 3-kinase signaling cascade. Cancer Res 2007;67:2736-2746.
37. Majumder S, Roy S, Kaffenberger T, Wang B, Costinean S, Frankel W, et al. Loss of metallothionein predisposes mice to diethylnitrosamine-induced hepatocarcinogenesis by activating NF-kappaB target genes. Cancer Res 2010;70:10265-10276.
38. Ghoshal K, Majumder S, Li Z, Dong X, Jacob ST. Suppression of metallothionein gene expression in a rat hepatoma because of promoter-specific DNA methylation. J Biol Chem 2000;275:539-547.
39. Harrington MA, Jones PA, Imagawa M, Karin M. Cytosine methylation does not affect binding of transcription factor Sp1. Proc Natl Acad Sci U S A 1988;85:2066-2070.
40. Li E, Beard C, Jaenisch R. Role for DNA methylation in genomic imprinting. Nature 1993;366:362-365.
41. Majumder S, Kutay H, Datta J, Summers D, Jacob ST, Ghoshal K. Epigenetic regulation of metallothionein-i gene expression: differential regulation of methylated and unmethylated promoters by DNA methyltransferases and methyl CpG binding proteins. J Cell Biochem 2006; 97:1300-1316.
42. Garzon R, Calin G, Croce C. MicroRNAs in cancer. Annu Rev Med 2009;60:167-179.
43. Merritt W, Lin Y, Han L, Kamat A, Spannuth W, Schmandt R, et al. Dicer, Drosha, and outcomes in patients with ovarian cancer. N Engl J Med 2008;359:2641-2650.
44. Horikawa Y, Wood CG, Yang H, Zhao H, Ye Y, Gu J, et al. Single nucleotide polymorphisms of microRNA machinery genes modify the risk of renal cell carcinoma. Clin Cancer Res 2008;14:7956-7962.
45. Yang H, Dinney CP, Ye Y, Zhu Y, Grossman HB, Wu X. Evaluation of genetic variants in microRNA-related genes and risk of bladder cancer. Cancer Res 2008;68:2530-2537.
46. Wu JM, Sheng H, Saxena R, Skill NJ, Bhat-Nakshatri P, Yu M, et al. NF-kappaB inhibition in human hepatocellular carcinoma and its potential as adjunct to sorafenib based therapy. Cancer Lett 2009;278: 145-155.
47. Gebhard C, Schwarzfischer L, Pham T, Andreesen R, Mackensen A, Rehli M. Rapid and sensitive detection of CpG-methylation using methyl-binding (MB)-PCR. Nucleic Acids Res 2006;34:e82.
48. Martello G, Rosato A, Ferrari F, Manfrin A, Cordenonsi M, Dupont S, et al. A microRNA targeting dicer for metastasis control. Cell 2010; 141:1195-1207.

J Gastroenterol (2013) 48:366–373
DOI 10.1007/s00535-012-0635-7

ORIGINAL ARTICLE—LIVER, PANCREAS, AND BILIARY TRACT

Perihepatic lymph node enlargement is a negative predictor of liver cancer development in chronic hepatitis C patients

Hiromi Hikita · Hayato Nakagawa · Ryosuke Tateishi · Ryota Masuzaki · Kenichiro Enooku · Haruhiko Yoshida · Masao Omata · Yoko Soroida · Mamiko Sato · Hiroaki Gotoh · Atsushi Suzuki · Tomomi Iwai · Hiromitsu Yokota · Kazuhiko Koike · Yutaka Yatomi · Hitoshi Ikeda

Received: 5 January 2012 / Accepted: 19 June 2012 / Published online: 12 July 2012

Abstract
Background Perihepatic lymph node enlargement (PLNE) is a common ultrasound finding in chronic hepatitis C patients. Although PLNE is considered to reflect the inflammatory response to hepatitis C virus (HCV), its clinical significance remains unclear.
Methods Between December 2004 and June 2005, we enrolled 846 chronic hepatitis C patients in whom adequate ultrasound examinations had been performed. PLNE was defined as a perihepatic lymph node that was at least 1 cm in the longest axis by ultrasonography. We analyzed the clinical features of patients with PLNE and prospectively investigated the association between PLNE and hepatocellular carcinoma (HCC) development.
Results We detected PLNE in 169 (20.0 %) patients. Female sex, lower body mass index (BMI), and HCV serotype 1 were independently associated with the presence of PLNE. However, there were no significant differences in liver function tests, liver stiffness, and hepatitis C viral loads between patients with and without PLNE. During the follow-up period (mean 4.8 years), HCC developed in 121 patients. Unexpectedly, patients with PLNE revealed a significantly lower risk of HCC development than those without PLNE ($p = 0.019$, log rank test). Multivariate analysis revealed that the presence of PLNE was an independent negative predictor of HCC development (hazard ratio 0.551, $p = 0.042$). In addition, the sustained viral response rate in patients who received interferon (IFN) therapy was significantly lower in patients with PLNE than in patients without PLNE.
Conclusions Patients with PLNE had a lower risk of HCC development than those without PLNE. This study may provide new insights into daily clinical practice and the pathophysiology of HCV-induced hepatitis and hepatocarcinogenesis.

Keywords Perihepatic lymph node enlargement · Chronic hepatitis C · Hepatocarcinogenesis

Abbreviations

ALT	Alanine aminotransferase
AFP	α-Fetoprotein
PLNE	Perihepatic lymph node enlargement
HCV	Hepatitis C virus
HCC	Hepatocellular carcinoma
IFN	Interferon
LN	Lymph node
US	Ultrasonography

Introduction

Hepatocellular carcinoma (HCC) is the fifth most common cancer worldwide and chronic hepatitis C virus (HCV)

H. Hikita and H. Nakagawa contributed equally to this work.

H. Hikita · H. Nakagawa · K. Enooku · Y. Soroida · M. Sato · H. Gotoh · A. Suzuki · T. Iwai · H. Yokota · Y. Yatomi · H. Ikeda
Department of Clinical Laboratory Medicine, Graduate School of Medicine, University of Tokyo, 7-3-1 Hongo, Bunkyo-ku, Tokyo 113-8655, Japan

H. Nakagawa (✉) · R. Tateishi · R. Masuzaki · K. Enooku · H. Yoshida · K. Koike · H. Ikeda
Department of Gastroenterology, Graduate School of Medicine, University of Tokyo, 7-3-1 Hongo, Bunkyo-ku, Tokyo 113-8655, Japan
e-mail: n-hayato@yf7.so-net.ne.jp

M. Omata
Yamanashi Prefectural Hospital Organization, 1-1-1 Fujimi, Kofu, Yamanashi 400-8506, Japan

infection is a major cause of HCC in the United States, southern European countries, and Japan [1, 2]. The host immune responses to HCV are often not strong enough to completely clear the infection, resulting in chronic stimulation of the antigen-specific immune response. Accumulating basic and clinical lines of evidence indicate that a sustained inflammatory reaction in the liver is the major contributing factor to HCC development [3–5].

Inflammatory processes in organs frequently lead to hyperplasia of regional lymph nodes (LNs). Perihepatic LN enlargement (PLNE) is a common finding in patients with chronic hepatitis, especially in patients with hepatitis C [6, 7]. Some studies have revealed that PLNE in chronic hepatitis C patients was associated with a higher HCV viral load, [7] higher histological grade of hepatic inflammation and fibrosis [8, 9], and higher CD8 lymphocyte level in the blood [10]; therefore, PLNE is considered to reflect an inflammatory response to HCV. However, such associations as those noted above are inconsistent among studies [7–15], and the precise mechanism and clinical relevance of PLNE are not fully understood. Furthermore, to our knowledge, there have been no studies designed to investigate the association between PLNE and hepatocarcinogenesis. To clarify whether we should pay attention to the risk of HCC development in patients with PLNE is very important, because we encounter such situations very often.

The purpose of this study was to reevaluate the clinical relevance of PLNE and to carry out a prospective assessment of the association between PLNE and HCC development. To elucidate these matters, we investigated a well-characterized chronic hepatitis C cohort in which we previously reported the utility of performing transient elastography for risk assessment of HCC development [16]. In the present study, we prospectively assessed the association between PLNE and HCC development in chronic hepatitis C patients in that cohort.

Patients and methods

Patients and screening for perihepatic LN enlargement

As described previously [16], we enrolled 866 chronic hepatitis C patients, excluding those with HCC or a past history of it, who visited the University of Tokyo Hospital between December 2004 and June 2005. All patients were positive for HCV-RNA and showed at least a transiently elevated serum alanine aminotransferase (ALT) level. Patients with concomitant hepatitis B virus surface antigen positivity, patients with uncontrollable ascites, patients on interferon (IFN) therapy, and patients who visited only for consultation purposes were excluded from this study.

Each subject was screened for HCC with ultrasonography (US) at or immediately after the first visit. At the same time, we surveyed the presence of PLNE with US. The US examination was performed using the SSD-2000 (Aloka, Tokyo, Japan). To identify LNs the following criteria were used, according to a previous report [17]: one or more masses with an ovoid shape and less echogenic than liver parenchyma, separated from adjacent organs and vessels by a clear-cut cleavage on repeated transverse, sagittal, and oblique scans. LNs were searched for near the trunk of the portal vein, hepatic artery, celiac axis, superior mesenteric vein, and pancreas head. Furthermore, we used Doppler US to differentiate LNs from vessels.

We defined PLNE as an LN that was at least 1 cm in the longest axis. There were two reasons for this definition. First, we preliminarily investigated the prevalence of PLNE with US in 465 healthy subjects who had had medical check-ups and did not have liver disease or other underlying causes of LN enlargement. We found that only 15 (3.2 %) of these subjects had a perihepatic LN larger than 1 cm in the longest axis (unpublished data). Second, when an LN was smaller than 1 cm, it was sometimes difficult to distinguish the LN from other structures. If two or more LNs were detected with US, we determined PLNE to be present based on the length of the largest LN. In 20 of the 866 patients in the present study, adequate visualization of the liver hilum was not achieved with US because of severe obesity or excessive meteorism. Therefore, we analyzed the association between PLNE and the subsequent incidence of HCC in 846 patients.

HCV RNA was measured using Amplicore HCV version 2.0 (Roche, Tokyo, Japan), and the HCV serotype was examined using a serotyping assay (SRL, Tokyo, Japan). We also monitored IFN therapy and responses during the follow-up period. A sustained virological response (SVR) was defined as undetectable HCV-RNA at least 24 weeks after the end of therapy. All blood tests were performed at the time of US examination.

The study protocol conformed to the ethical guidelines of the 1975 Declaration of Helsinki.

Patient follow up

Patients were followed up every 3–6 months at the outpatient clinic, when blood tests (including tumor markers) and US were carried out. Contrast-enhanced computed tomography (CT) was performed when HCC was suspected, based on US, and/or if the serum α-fetoprotein (AFP) level showed an abnormal increase. HCC was diagnosed by dynamic CT, and hyperattenuation in the arterial phase with washout in the late phase was considered a definite sign of HCC [18]. When a diagnosis of HCC was ambiguous, ultrasound-guided tumor biopsy was

performed and a pathologic diagnosis was made based on the Edmondson and Steiner criteria. Time to HCC occurrence was defined as the interval between the date of the first US screening and the diagnosis of HCC. Patients were censored at the time of death without HCC development, the last visit when lost to follow up, or the end of the study period. The last observation in this study was made on December 31, 2010. Thus, the time of observation was extended from that of our previous study, which was censored on May 31, 2008 [16].

Transient elastography

Transient elastography was performed using Fibroscan (Echosens, Paris, France) as described previously [16].

Statistical analysis

Data were expressed as means ± standard deviation (SD) unless otherwise indicated. Categorical variables were compared by χ^2tests, whereas continuous variables were compared by the unpaired Student's *t*-test (parametric) or the Mann–Whitney *U*-test (non-parametric). Multivariate logistic regression analysis was used to identify factors that were independently associated with the presence of PLNE. Cumulative HCC incidence was estimated using the Kaplan–Meier method, and the difference between groups was assessed with the log-rank test. In the analysis of risk factors for hepatocarcinogenesis, we tested the following variables in univariate analysis and multivariate Cox proportional hazard regression analysis: age, sex, platelet count, serum albumin concentration, total bilirubin concentration, ALT and aspartate aminotransferase (AST) levels, higher AFP concentration (>10 ng/ml), prothrombin activity, heavy alcohol drinking (alcohol intake >80 g/day), BMI, higher liver stiffness measurement (LSM) (>10 kPa), HCV serotype, HCV viral load (>100 kIU/ml), IFN treatment, achievement of SVR, and presence of PLNE. A *p* value of less than 0.05 on a two-tailed test was considered significant. Data processing and analysis were performed using StatView (ver. 5.0; SAS Institute, Cary, NC, USA) and SPSS (ver. 14.0; SPSS, Chicago, IL, USA) software.

Results

Patient profiles

We detected PLNE in 169 of 846 (20.0 %) patients with chronic hepatitis C. A representative ultrasound image is shown in Fig. 1. The mean (±SD) length of the longest axis was 1.7 (±0.5) cm (range 1.0–3.5 cm). The clinical features of patients with and without PLNE are summarized in Table 1. The proportion of females was significantly higher in the PLNE-positive group than in the PLNE-negative group (63.3 vs. 52.9 %), and BMI was slightly but significantly lower in the PLNE-positive group than in the PLNE-negative group (21.9 ± 2.6 vs. 22.5 ± 2.9). The proportion of HCV serotype 1 patients was higher in the PLNE-positive group than in the PLNE-negative group, with borderline significance. There was a tendency of a higher serum ALT level in the PLNE-positive group, but the difference was without statistical significance. There were no significant differences in other liver function test results, or in liver stiffness and hepatitis C viral load between the two groups. Multivariate logistic regression analysis using the factors of sex, serum ALT, BMI, and HCV serotype revealed that female sex, lower BMI, and HCV serotype 1 were independently associated with the presence of PLNE (Table 2).

Incidence of HCC

The mean follow-up period was 4.8 years, constituting a total observation of 4,021 person-years. During the observation period, 70 (8.3 %) patients were lost to follow up: 15 (8.8 %) patients in the PLNE-positive group and 55 (8.1 %) patients in the PLNE-negative group. There were no patients in whom an enlarged perihepatic LN turned out to be caused by other underlying diseases including metastasis of HCC. The SVR rate in patients who received IFN therapy during the follow-up period was significantly lower in the PLNE-positive group compared with that in the PLNE-negative group [7/34 (20.6 %) vs. 93/172

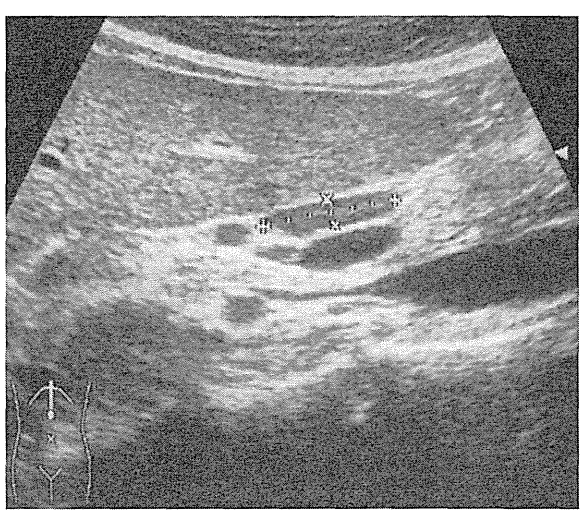

Fig. 1 Representative ultrasound image of enlarged perihepatic lymph node (LN) in a patient with chronic hepatitis C

Table 1 Clinical features of patients with and without PLNE

Variable	PLNE-positive group ($n = 169$)	PLNE-negative group ($n = 677$)	p value
Age (years)	62.4 ± 10.1 (29–83)	62.4 ± 11.5 (17–89)	0.58
Male, n (%)	62 (36.7)	319 (47.1)	0.018
Serum albumin (g/dl)	4.0 ± 0.4 (2.8–4.8)	4.0 ± 0.4 (2.5–5.0)	0.93
Total bilirubin (mg/dl)	0.8 ± 0.3 (0.3–2.1)	0.9 ± 0.5 (0.3–4.6)	0.23
AST (IU/l)	52 ± 34.1 (17–223)	50 ± 33.8 (9–286)	0.16
ALT (IU/l)	57 ± 48.7 (4–374)	53 ± 45.2 (2–503)	0.10
Platelet count ($\times 10^4/\mu l$)	16.1 ± 6.6 (2.1–42.2)	16.1 ± 6.7 (3.2–43.6)	0.89
Prothrombin time (%)	86.0 ± 12.1 (50.3–100.0)	85.7 ± 12.4 (38.9–100.0)	0.88
AFP (ng/ml)	22.0 ± 67.9 (1–592)	13.4 ± 37.1 (1–563)	0.61
BMI (kg/m^2)	21.9 ± 2.6 (14.4–28.7)	22.5 ± 2.9 (15.1–29.8)	0.007
Liver stiffness (kPa)	10.9 ± 7.8 (2.8–42.2)	12.0 ± 10.0 (2.5–75.0)	0.59
Alcohol consumption >80 g/day, n (%)	6 (3.6)	25 (3.7)	0.82
HCV viral load (kIU/ml)	549 ± 646 (5–5000)	651 ± 842 (5–5000)	0.48
HCV serotype 1, n (%)	146 (86.3)	538 (79.5)	0.053
Patients who received IFN, n (%)	34 (20.1)	172 (25.4)	0.18
Patients who achieved SVR, n (%)	7 (4.1)	93 (13.7)	0.0009

PLNE perihepatic lymph node enlargement, *AST* aspartate aminotransferase. *ALT* alanine aminotransferase, *AFP* α-fetoprotein, *BMI* body mass index, *HCV* hepatitis C virus

Table 2 Factors associated with the presence of PLNE: multivariate analysis

Variable	Odds ratio (95 % confidence interval [CI])	p value
Male sex	0.667 (0.464–0.936)	0.024
ALT level (per 1 IU/l)	1.003 (0.999–1.006)	0.10
BMI (per 1 kg/m^2)	0.919 (0.864–0.978)	0.017
HCV serotype 1	1.64 (1.02–2.66)	0.043

(54.1 %), $p = 0.0005$]. This finding was consistent with previous reports [12, 19].

By the end of the follow-up period, HCC had developed in 121 patients (3.0 % per 1 person-year). The cumulative incidence rates of HCC at 3 and 5 years estimated by the Kaplan–Meier method were 8.9 and 13.7 %, respectively. We then assessed the incidence of HCC stratified by the presence of PLNE. Unexpectedly, the PLNE-positive group revealed a significantly lower incidence of HCC than the PLNE-negative group ($p = 0.019$, log-rank test) (Fig. 2). The cumulative incidence rates at 3 and 5 years were 3.6 and 8.2 %, respectively, in the PLNE-positive group, and 10.1 and 15.1 % in the PLNE-negative group. These results indicate that patients with PLNE have a lower risk of HCC development despite having a lower SVR rate with IFN therapy.

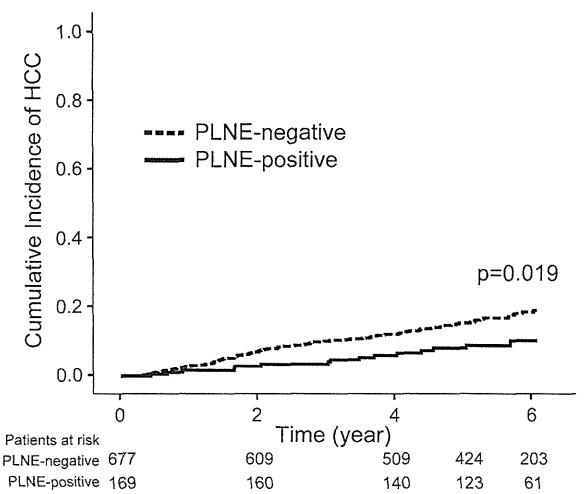

Fig. 2 Cumulative incidence of hepatocellular carcinoma (*HCC*) development stratified by the presence of perihepatic lymph node enlargement (*PLNE*)

Risk analyses

We analyzed the risk factors for HCC development. In the univariate analyses, older age, male sex, lower serum albumin concentration, higher total bilirubin concentration, higher AST level, higher ALT level, lower prothrombin activity, lower platelet count, heavy alcohol drinking, higher BMI, LSM greater than 10 kPa, AFP level greater than 10 ng/ml, HCV serotype 1, not receiving IFN, not achieving SVR, and absence of PLNE were significant risk factors for HCC (Table 3). As we had reported previously, a higher LSM (i.e., greater than 10 kPa) was a strong predictor of HCC development [hazard ratio (HR) 15.4, 95 % confidence interval (CI) 8.6–27.0, $p < 0.0001$)]. Multivariate proportional hazard regression analyses

Table 3 Risk factors for HCC development: univariate and multivariate analyses

Variable	Univariate analysis		Multivariate analysis	
	Hazard ratio (95 % CI)	*p* value	Hazard ratio (95 % CI)	*p* value
Age (per 1 year age)	1.07 (1.05–1.09)	<0.0001	1.04 (1.01–1.06)	0.002
Male sex	1.45 (1.02–2.08)	0.041	1.49 (1.02–2.17)	0.039
Platelet count (per $10^4/\mu l$)	0.852 (0.823–0.882)	<0.0001	0.965 (0.926–1.005)	0.089
Total bilirubin (per 1 mg/dl)	1.88 (1.45–2.45)	<0.0001	0.825 (0.567–1.2)	0.32
Serum albumin level (per 1 g/dl)	0.12 (0.084–0.17)	<0.0001	0.441 (0.263–0.739)	0.002
AST level (per 1 IU/l)	1.01 (1.007–1.014)	<0.0001	1.002 (0.991–1.013)	0.71
ALT level (per 1 IU/l)	1.004 (1.002–1.007)	0.002	1.0 (0.991–1.013)	0.94
AFP level >10 ng/ml	6.76 (4.69–9.8)	<0.0001	1.9 (1.22–2.97)	0.005
Prothrombin time (per 1 %)	0.973 (0.966–0.979)	<0.0001	0.989 (0.976–1.001)	0.072
Alcohol consumption >80 g/day	2.73 (1.43–5.24)	0.002	3.53 (1.76–7.09)	0.0004
BMI (per 1 kg/m^2)	1.09 (1.03–1.16)	0.006	1.09 (1.01–1.17)	0.025
Liver stiffness >10 kPa	15.4 (8.6–27.0)	<0.0001	4.41 (2.24–8.7)	<0.0001
HCV serotype 1	1.76 (1.03–3.03)	0.04	1.36 (0.774–2.38)	0.29
HCV-RNA >100 kIU/ml	1.36 (0.87–2.13)	0.18	1.24 (0.781–1.97)	0.36
Patients treated with IFN	0.44 (0.262–0.75)	0.002	0.59 (0.315–1.11)	0.1
Patients with SVR	0.175 (0.055–0.549)	0.003	0.621 (0.169–2.28)	0.47
Presence of PLNE	0.53 (0.31–0.91)	0.02	0.551 (0.31–0.978)	0.042

HCC hepatocellular carcinoma, *IFN* interferon, *SVR* sustained viral response

revealed that older age, male sex, lower serum albumin concentration, AFP level greater than 10 ng/ml, heavy alcohol drinking, higher BMI, LSM greater than 10 kPa, and absence of PLNE were independent risk factors for HCC (Table 3). These results suggest that the presence of PLNE is an independent negative predictor of HCC development in chronic hepatitis C patients.

Subgroup analysis of non-obese patients

To further rule out the possibility that obesity acted as a confounder in the association between the presence of PLNE and HCC development, we reanalyzed the contribution of PLNE to HCC development in a subgroup of non-obese patients, defined as those with BMI <25 kg/m^2 ($n = 695$), because we could clearly visualize the liver hilum in such individuals. As shown in Fig. 3, the PLNE-positive group had a significantly lower incidence of HCC than the PLNE-negative group even in the non-obese subgroup ($p = 0.02$). Thus, we further confirmed that the presence of PLNE was negatively associated with HCC development independently of obesity.

Significance of the size of perihepatic LNs

To examine the significance of the size of perihepatic LNs, we divided patients with PLNE into two groups: a smaller LN group (longest axis of LN 1 cm to 2 cm, $n = 122$) and a larger LN group (longest axis of LN ≥2 cm, $n = 47$).

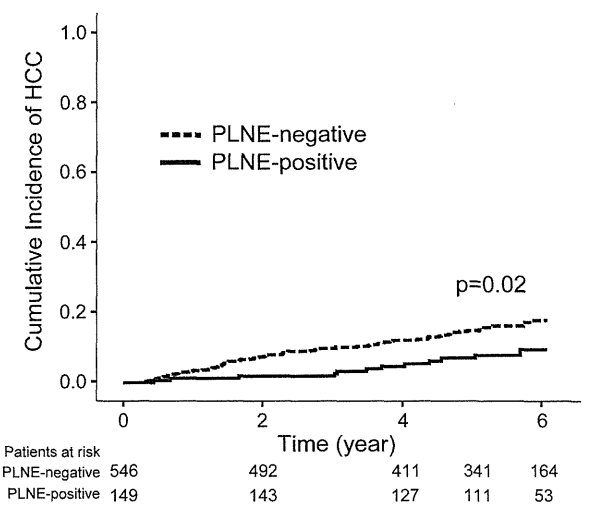

Fig. 3 Cumulative incidence of HCC development stratified by the presence of PLNE: subgroup analysis of non-obese patients (body mass index [BMI] <25 kg/m^2)

The characteristics of each group are summarized in Table 4. The proportion of male patients and the LSM value tended to be higher in the larger LN group than in the smaller LN group, but the difference was not statistically significant for either factor. There were no significant differences in other factors between the two groups. Furthermore, there was no significant difference in HCC incidence rates between the two groups (Fig. 4), although the larger LN group revealed a slightly higher incidence of

Table 4 Comparison of clinical features between patients with small perihepatic lymph nodes (LNs) and those with large perihepatic LNs

Variable	LN size 1 cm to <2 cm, (n = 122)	LN size ≥2 cm (n = 47)	p value
Age (years)	62.7 ± 10.4 (29–83)	61.5 ± 9.2 (32–77)	0.32
Male, n (%)	40 (32.8)	22 (46.8)	0.092
Serum albumin (g/dl)	4.0 ± 0.3 (3.0–4.8)	4.0 ± 0.4 (2.8–4.8)	0.96
Total bilirubin (mg/dl)	0.8 ± 0.3 (0.3–1.6)	0.8 ± 0.4 (0.3–2.1)	0.98
AST (IU/l)	53 ± 36.0 (17–223)	50 ± 28.7 (17–181)	0.83
ALT (IU/l)	56 ± 49.0 (4–374)	59 ± 48.2 (6–308)	0.48
Platelet count ($\times 10^4/\mu l$)	16.3 ± 6.2 (2.1–36.4)	15.4 ± 7.4 (4.8–42.2)	0.25
Prothrombin time (%)	86.7 ± 11.7 (57.4–100.0)	84.2 ± 13.0 (50.3–100.0)	0.27
AFP (ng/ml)	13.0 ± 27.7 (1–168)	45.3 ± 118.6 (1–592)	0.19
BMI (kg/m^2)	21.8 ± 2.6 (16.8–28.0)	22.0 ± 2.6 (14.4–28.7)	0.75
Liver stiffness (kPa)	10.2 ± 7.1 (2.8–37.4)	12.5 ± 9.3 (4.2–42.2)	0.064
Alcohol consumption >80 g/day, n (%)	5 (4.1)	1 (2.1)	0.54
HCV viral load (kIU/ml)	658 ± 788	504 ± 582	0.17
HCV serotype 1, n (%)	107 (87.7)	39 (83.0)	0.58
Patients who received IFN, n (%)	24 (19.6)	10 (21.2)	0.98
Patients who achieved SVR, n (%)	5 (4.1)	2 (4.3)	0.99

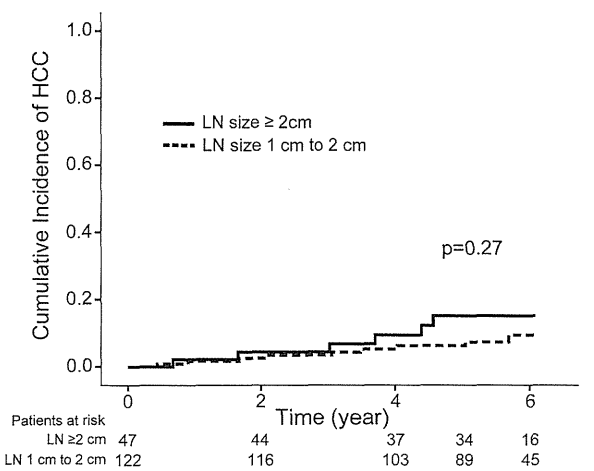

Fig. 4 Cumulative incidence of HCC development in patients with PLNE stratified by the size of perihepatic LNs: i.e., smaller (longest axis of LN 1 to <2 cm) and larger (longest axis of LN ≥2 cm)

HCC. These results suggest that the size of perihepatic LNs in chronic hepatitis C patients may not be clinically as important as the presence of PLNE itself.

Discussion

Although PLNE is a common finding in patients with chronic hepatitis C, its clinical significance has remained unclear. In the present study, we reevaluated the clinical relevance of PLNE in a large cohort of chronic hepatitis C patients. We found, by prospective analysis, that patients with PLNE had a lower risk of HCC development than those without PLNE. To our knowledge, this is the first study reporting a negative association between the presence of PLNE and HCC development.

Before we started this study, we expected that patients with PLNE would have a higher risk of HCC development, based on previous reports showing positive associations between PLNE and liver inflammation and fibrosis [8, 13–15]. However, in our study, neither inflammatory markers, such as serum AST and ALT levels, nor fibrosis markers, such as the platelet count and LSM, had statistically significant associations with the presence of PLNE. On the contrary, patients with PLNE revealed a significantly lower risk of HCC development. One possible explanation for this result is that obesity may affect the ability of US to detect perihepatic LNs, although patients with severe obesity were excluded from the study. To rule out the effect of confounders, especially obesity, we performed multivariate analysis and subgroup analysis of non-obese patients, and the results showed that the presence of PLNE was an independent negative predictor of HCC development. Additionally, of the 846 patients enrolled in this study, 175 patients underwent abdominal computed tomography (CT) within one year from the date of the US examination. The concordance rate for the diagnosis of PLNE between CT and US in these patients was 91.4 % (160/175). Therefore, we consider that the diagnostic accuracy of US for PLNE was acceptable in this study.

Although the mechanism of PLNE in patients with hepatitis C is still unknown, hyperplasia of regional LNs is generally considered to reflect inflammatory responses in the adjacent organs. The volume of perihepatic LNs has been reported to significantly decrease after antiviral

therapy, especially in patients with an SVR, supporting the hypothesis that PLNE reflects the inflammatory response to HCV [19–21]. In fact, PLNE was reported to be associated with CD8 lymphocyte counts in the peripheral blood [10]. Furthermore, HCV-specific IFN-γ production and proliferative responses of T cells were found most commonly in perihepatic LNs rather than in liver tissue or in the peripheral blood, indicating that there was ongoing T-cell activation in perihepatic LNs [22]. Our results, taken together with these previous reports, suggest that the presence of PLNE may reflect an adequate host immune response to HCV. T-cell immunity is very important in the control of HCV infection and in the prevention of hepatocarcinogenesis [23–25], and a T-cell response that is too weak may accelerate hepatocarcinogenesis, as seen in patients co-infected with HCV and human immunodeficiency virus [26, 27]. Thus, a weak T-cell response may be one explanation of the higher risk of HCC development in patients without PLNE. On the other hand, too strong an anti-HCV T-cell response may induce hepatocellular damage and lead to subsequent hepatocarcinogenesis [28], so patients with larger perihepatic LNs may have a slightly higher tendency to develop HCC. However, from the present type of observational study, we cannot evaluate a causal relationship between PLNE and hepatocarcinogenesis, so further studies are needed to clarify this point.

As mentioned above, several studies have shown that PLNE was positively associated with the degree of liver inflammation or fibrosis [8, 13–15], but, in the present study we could not find such associations, except for slight serum ALT elevation. However, because of ethical concerns regarding the performance of liver biopsy, we did not assess liver histology, so we cannot conclude whether or not PLNE is really associated with liver inflammation and fibrosis. Of note, the reported relationships of PLNE to liver function tests and liver inflammation and fibrosis are inconsistent among studies [7–15]. One reason may be that these findings were based on relatively small samples. Another reason is that there is a lack of established criteria for the diagnosis of PLNE. The lack of definite criteria may also contribute to the wide variation in the prevalence of PLNE among studies (from 20 to 100 %) [8–10, 21]. We defined PLNE as an LN that was at least 1 cm in the longest axis, and this definition was based on the report by Grier et al. [21] and our preliminary investigation in healthy subjects. Some studies have used more detailed measurements of LNs with calculations of node volume and shape [8, 10, 20]. These methods are certainly more accurate in terms of the assessment of nodal volume, but may be too complicated in the clinical setting, as discussed by Grier et al. [21]. We used a simpler method, because our study included a large number of patients and was conducted to examine the significance of PLNE in daily clinical practice. Admittedly, a more detailed method would be appropriate to elucidate more clearly the involvement of PLNE in the pathophysiology of hepatitis and hepatocarcinogenesis.

In the present study, female sex, lower BMI, and HCV serotype 1 were independently associated with the presence of PLNE. Soresi et al. [29] also reported that PLNE was observed significantly more often in female patients than in male patients with chronic hepatitis C. Although we cannot clarify the mechanism underlying this association, this finding may be interesting from the point of view of gender differences in immune systems and hepatocarcinogenesis. In the study by Soresi et al., BMI in patients with PLNE tended to be lower than that in patients without PLNE, although the difference was not statistically significant [29], and this finding may be in line with our present results. Regarding BMI in patients with chronic HCV infection, an anti-HCV specific immune response was reportedly associated with lower BMI through the expression of adiponectin, one of the major adipokines [30]. Thus, the active immune response to HCV in patients with lower BMI might cause PLNE. Recent studies have reported that obesity and obesity-induced dysregulation of adipokines play important roles in hepatocarcinogenesis [31–33], so the examination of adipokine expression may help to explain the relationship of PLNE to BMI and hepatocarcinogenesis.

Another important finding in our study was that the SVR rate in patients who received IFN therapy was significantly lower in patients with PLNE than in patients without PLNE. This finding is consistent with previous reports [12, 19]. Although the proportion of individuals with HCV serotype 1 was higher in our patients with PLNE than in patients without PLNE, subgroup analysis of the patients with HCV serotype 1 also revealed a significantly lower SVR rate in patients with PLNE than in patients without PLNE (data not shown). Therefore, further analyses are planned to clarify the relationship of PLNE to HCV serotype and response to IFN therapy.

In conclusion, the presence of PLNE is an independent negative predictor of HCC development in chronic hepatitis C patients. This study may provide new insights into daily clinical practice and the pathophysiology of HCV-induced hepatitis and hepatocarcinogenesis.

Acknowledgments This study was not supported by any grants.

Conflict of interest The authors have no conflicts of interest regarding this study.

References

1. Bosch FX, Ribes J, Diaz M, Cleries R. Primary liver cancer: worldwide incidence and trends. Gastroenterology. 2004;127: S5–16.

2. El-Serag HB, Rudolph KL. Hepatocellular carcinoma: epidemiology and molecular carcinogenesis. Gastroenterology. 2007;132:2557–76.
3. Levrero M. Viral hepatitis and liver cancer: the case of hepatitis C. Oncogene. 2006;25:3834–47.
4. Berasain C, Castillo J, Perugorria MJ, Latasa MU, Prieto J, Avila MA. Inflammation and liver cancer: new molecular links. Ann N Y Acad Sci. 2009;1155:206–21.
5. Nakagawa H, Maeda S, Yoshida H, Tateishi R, Masuzaki R, Ohki T, et al. Serum IL-6 levels and the risk for hepatocarcinogenesis in chronic hepatitis C patients: an analysis based on gender differences. Int J Cancer. 2009;125:2264–9.
6. Kuo HT, Lin CY, Chen JJ, Tsai SL. Enlarged lymph nodes in porta hepatis: sonographic sign of chronic hepatitis B and C infections. J Clin Ultrasound. 2006;34:211–6.
7. Watanabe T, Sassa T, Hiratsuka H, Hattori S, Abe A. Clinical significance of enlarged perihepatic lymph node on ultrasonography. Eur J Gastroenterol Hepatol. 2005;17:185–90.
8. Dietrich CF, Lee JH, Herrmann G, Teuber G, Roth WK, Caspary WF, et al. Enlargement of perihepatic lymph nodes in relation to liver histology and viremia in patients with chronic hepatitis C. Hepatology. 1997;26:467–72.
9. Soresi M, Carroccio A, Bonfissuto G, Agate V, Magliarisi C, Aragona F, et al. Ultrasound detection of abdominal lymphadenomegaly in subjects with hepatitis C virus infection and persistently normal transaminases: a predictive index of liver histology severity. J Hepatol. 1998;28:544–9.
10. Muller P, Renou C, Harafa A, Jouve E, Kaplanski G, Ville E, et al. Lymph node enlargement within the hepatoduodenal ligament in patients with chronic hepatitis C reflects the immunological cellular response of the host. J Hepatol. 2003;39:807–13.
11. Cassani F, Valentini P, Cataleta M, Manotti P, Francesconi R, Giostra F, et al. Ultrasound-detected abdominal lymphadenopathy in chronic hepatitis C: high frequency and relationship with viremia. J Hepatol. 1997;26:479–83.
12. del Olmo JA, Esteban JM, Maldonado L, Rodriguez F, Escudero A, Serra MA, et al. Clinical significance of abdominal lymphadenopathy in chronic liver disease. Ultrasound Med Biol. 2002;28:297–301.
13. Tavakoli-Tabasi S, Ninan S. Clinical significance of perihepatic lymphadenopathy in patients with chronic hepatitis C infection. Dig Dis Sci. 2011;56:2137–44.
14. Soresi M, Carroccio A, Agate V, Bonfissuto GD, Magliarisi C, Fulco M, et al. Evaluation by ultrasound of abdominal lymphadenopathy in chronic hepatitis C. Am J Gastroenterol. 1999;94:497–501.
15. Soresi M, Bonfissuto G, Magliarisi C, Riili A, Terranova A, Di Giovanni G, et al. Ultrasound detection of abdominal lymph nodes in chronic liver diseases. A retrospective analysis. Clin Radiol. 2003;58:372–7.
16. Masuzaki R, Tateishi R, Yoshida H, Goto E, Sato T, Ohki T, et al. Prospective risk assessment for hepatocellular carcinoma development in patients with chronic hepatitis C by transient elastography. Hepatology. 2009;49:1954–61.
17. Cassani F, Zoli M, Baffoni L, Cordiani MR, Brunori A, Bianchi FB, et al. Prevalence and significance of abdominal lymphadenopathy in patients with chronic liver disease: an ultrasound study. J Clin Gastroenterol. 1990;12:42–6.
18. Bruix J, Sherman M. Management of hepatocellular carcinoma. Hepatology. 2005;42:1208–36.
19. Friedrich-Rust M, Forestier N, Sarrazin C, Reesink HW, Herrmann E, Zeuzem S. Ultrasound evaluation of perihepatic lymph nodes during antiviral therapy with the protease inhibitor telaprevir (VX-950) in patients with chronic hepatitis C infection. Ultrasound Med Biol. 2007;33:1362–7.
20. Dietrich CF, Stryjek-Kaminska D, Teuber G, Lee JH, Caspary WF, Zeuzem S. Perihepatic lymph nodes as a marker of antiviral response in patients with chronic hepatitis C infection. AJR Am J Roentgenol. 2000;174:699–704.
21. Grier S, Patel N, Kuo YT, Cosgrove DO, Goldin RC, Thomas HC, et al. Perihepatic lymph nodes as markers of disease response in patients with hepatitis C-related liver disease: a prospective clinical evaluation. Eur J Gastroenterol Hepatol. 2010;22:257–63.
22. Moonka D, Milkovich KA, Rodriguez B, Abouljoud M, Lederman MM, Anthony DD. Hepatitis C virus-specific T-cell gamma interferon and proliferative responses are more common in perihepatic lymph nodes than in peripheral blood or liver. J Virol. 2008;82:11742–8.
23. Bowen DG, Walker CM. Adaptive immune responses in acute and chronic hepatitis C virus infection. Nature. 2005;436:946–52.
24. Nakagawa H, Hirata Y, Takeda K, Hayakawa Y, Sato T, Kinoshita H, et al. Apoptosis signal-regulating kinase 1 inhibits hepatocarcinogenesis by controlling the tumor-suppressing function of stress-activated mitogen-activated protein kinase. Hepatology. 2011;54:185–95.
25. Kang TW, Yevsa T, Woller N, Hoenicke L, Wuestefeld T, Dauch D, et al. Senescence surveillance of pre-malignant hepatocytes limits liver cancer development. Nature. 2011;479:547–51.
26. Garcia-Samaniego J, Rodriguez M, Berenguer J, Rodriguez-Rosado R, Carbo J, Asensi V, et al. Hepatocellular carcinoma in HIV-infected patients with chronic hepatitis C. Am J Gastroenterol. 2001;96:179–83.
27. Brau N, Fox RK, Xiao P, Marks K, Naqvi Z, Taylor LE, et al. Presentation and outcome of hepatocellular carcinoma in HIV-infected patients: a US—Canadian multicenter study. J Hepatol. 2007;47:527–37.
28. Maeda S. NF-kappaB, JNK, and TLR signaling pathways in hepatocarcinogenesis. Gastroenterol Res Pract. 2010;2010:367694.
29. Soresi M, Bonfissuto G, Sesti R, Riili A, Di Giovanni G, Carroccio A, et al. Perihepatic lymph nodes and antiviral response in chronic HCV-associated hepatitis. Ultrasound Med Biol. 2004;30:711–7.
30. Palmer C, Hampartzoumian T, Lloyd A, Zekry A. A novel role for adiponectin in regulating the immune responses in chronic hepatitis C virus infection. Hepatology. 2008;48:374–84.
31. Ohki T, Tateishi R, Shiina S, Goto E, Sato T, Nakagawa H, et al. Visceral fat accumulation is an independent risk factor for hepatocellular carcinoma recurrence after curative treatment in patients with suspected NASH. Gut. 2009;58:839–44.
32. Park EJ, Lee JH, Yu GY, He G, Ali SR, Holzer RG, et al. Dietary and genetic obesity promote liver inflammation and tumorigenesis by enhancing IL-6 and TNF expression. Cell. 2010;140:197–208.
33. Arano T, Nakagawa H, Tateishi R, Ikeda H, Uchino K, Enooku K, et al. Serum level of adiponectin and the risk of liver cancer development in chronic hepatitis C patients. Int J Cancer. 2011;129:2226–35.

J Gastroenterol (2013) 48:254–268
DOI 10.1007/s00535-012-0631-y

ORIGINAL ARTICLE—LIVER, PANCREAS, AND BILIARY TRACT

Meta-analysis: mortality and serious adverse events of peginterferon plus ribavirin therapy for chronic hepatitis C

Tatsuya Minami · Takahiro Kishikawa · Masaya Sato · Ryosuke Tateishi · Haruhiko Yoshida · Kazuhiko Koike

Received: 9 February 2012 / Accepted: 11 June 2012 / Published online: 12 July 2012

Abstract
Background Pegylated interferon (PEG-IFN) plus ribavirin (RBV) therapy is the current standard of care for patients with chronic hepatitis C. Determining precisely the risk of serious adverse events (SAEs) and mortality from a single study is rather difficult because of the infrequency of such events. The aim of this systematic review was to assess the rates of SAEs and the mortality of PEG-IFN/RBV therapy in a pooled large sample, and to assess the relationship between SAEs and mortality rates and therapeutic characteristics.
Methods A literature search was conducted using MEDLINE, EMBASE, and the Cochrane Library to identify randomized controlled trials evaluating the efficacy and safety of PEG-IFN/RBV therapy. We calculated the crude mortality and SAE rates with 95 % confidence intervals (CIs).
Results Eighty studies with 153 treatment arms that included 27569 patients were enrolled (14401 patients treated with Peg-IFN alpha-2a/RBV and 13168 with Peg-IFN alpha-2b/RBV). All-cause and treatment-related deaths were observed in 50 (0.18 %; 95 % confidence interval [CI] 0.13–0.24 %) and sixteen (0.058 %; 95 % CI 0.033–0.094 %) patients, respectively. The crude SAE rate was 7.08 % (95 % CI 6.75–7.41 %). Subgroup analysis revealed higher SAE rates in patients receiving PEG-IFN alpha-2a than in those with PEG-IFN alpha-2b (7.45 vs. 6.74 %), and higher SAE rates with higher doses than with the lower doses in PEG-IFN-2a and 2b (11.94 vs. 6.99 %, 7.10 vs. 5.05 %, respectively), and with extended duration (>48 weeks) than with standard duration (48 weeks) (15.5 vs. 6.67 %) in PEG-IFN alpha-2a.
Conclusion The mortality rate during PEG-IFN/RBV therapy was acceptably low, but the rate of SAEs was not negligible in a treatment for a benign disease, and the rate was affected by treatment regimens.

Keywords Peginterferon · Ribavirin · Hepatitis C · Mortality · Adverse event · Systematic review

Abbreviations

CI	Confidence interval
HCV	Hepatitis C virus
HCC	Hepatocellular carcinoma
PEG-IFN	Pegylated interferon
RCT	Randomized controlled trial
RBV	Ribavirin
SAE	Serious adverse event
SVR	Sustained virological response
WHO	World Health Organization

Introduction

Chronic hepatitis C virus (HCV) infection affects more than 170 million people worldwide and is a major cause of cirrhosis and hepatocellular carcinoma (HCC) [1, 2]. Currently the standard of care for patients with chronic hepatitis C is peginterferon (PEG-IFN) plus ribavirin (RBV) therapy,

Electronic supplementary material The online version of this article (doi:10.1007/s00535-012-0631-y) contains supplementary material, which is available to authorized users.

T. Minami · T. Kishikawa · M. Sato · R. Tateishi (✉) · H. Yoshida · K. Koike
Department of Gastroenterology, Graduate School of Medicine, The University of Tokyo, 7-3-1 Hongo, Bunkyo-ku, Tokyo 113-8655, Japan
e-mail: tateishi-tky@umin.ac.jp

which can induce a sustained virological response (SVR) in 40–50 % of treatment-naïve patients with genotype 1 and an SVR of approximately 80 % in treatment-naïve patients with genotypes 2 or 3 [3–8]. After an SVR is achieved, the risk of developing liver failure and HCC is greatly reduced [9]. However, this treatment is associated with various types of complications, some of which lead to fatal outcomes. Because death during treatment is a rare event, a large sample size is needed to accurately assess the mortality rate and risk factors. The aim of this systematic review was to assess the rates of serious adverse events (SAEs) and mortality during PEG-IFN/RBV therapy in a pooled large-sized sample and to assess the relationship between mortality and SAE rates and therapeutic characteristics.

Methods

Study search protocol

We searched MEDLINE, EMBASE, and the Cochrane Library to identify randomized controlled trials (RCTs) evaluating the efficacy and safety of PEG-IFN/RBV therapy published between December 1999 and October 2010. We used the following search terms: *chronic hepatitis C*, *interferon*, and *pegylated* or *peg* or *peginterferon* or *pegasys* or *pegintron*. The search was limited to the English language.

Inclusion criteria

Studies were included in the analysis if: (1) they were RCTs, (2) they included at least one PEG-IFN/RBV treatment group in patients with chronic hepatitis C, (3) they clearly specified adverse events, (4) patients were followed up until at least 24 weeks after the end of treatment, and (5) the studies had been published or accepted for publication as full-length articles. Studies were excluded if: (1) they dealt only with co-infection of HCV and HIV; (2) they dealt only with patients with a specific condition such as a comorbid disease (e.g., cryoglobulinemia), status after liver transplantation, or patients on dialysis; (3) they included patients under 18 years of age; or (4) they focused on specific adverse events or only on hemodynamic status. We restricted the included studies to RCTs on the premise that the quality of RCTs is superior to that of non-randomized or retrospective studies.

Data extraction

Two authors (T. M. and T. K.) independently screened titles and abstracts for potential eligibility and the full texts for final eligibility. Disagreements were resolved by consensus or by consulting a third author (R. T.). We extracted the data using a standardized data-collection form to record details of the study design, treatment doses and duration, number of patients in the arm, patient characteristics, and outcomes. A database using Microsoft Access 2010 (Microsoft, Redmond, WA, USA) was developed specifically for that purpose. Two authors independently entered data into the form, and the data were then compared. Any discrepancies were checked and resolved by consensus.

Statistical analysis

The primary and secondary outcome measures were mortality and SAE rates during PEG-IFN/RBV therapy, respectively. We recorded the number of SAEs and deaths observed in each arm of the included studies. We calculated crude mortality and SAE rates with 95 % confidence intervals (CI) by dividing the total number of deaths or SAEs observed by the total number of patients in the relevant group. Studies that did not discriminate serious adverse events from others were not included in the analyses of the corresponding outcome. We performed a subgroup analysis by comparing mortality and SAE rates between PEG-IFN alpha-2a and alpha-2b, high-dose and low-dose PEG-IFN, and shorter and longer treatment durations. We also performed a meta-regression analysis to investigate relationships between mortality and SAE rates and continuous variables (mean age; mean body weight; proportion of males; proportion of Caucasian, African, and Asian patients; and proportion of genotype 1 patients) using the random effects model. Heterogeneity was tested using the I^2 test to calculate the percentage of variation caused by heterogeneity rather than by chance alone [10]. The analyses were performed with S-plus Ver. 7.0 (Insightful, Seattle, WA, USA) and StatsDirect version 2.7.7 (StatsDirect, Chesire, UK). The threshold of the reported P value accepted as indicating significance was <0.05.

Results

Study characteristics

Figure 1 shows the results of the screening. Our initial database search retrieved 323 citations, of which 243 were excluded because they did not meet our inclusion criteria; therefore, a total of 80 RCTs with 153 arms that included 27569 patients were enrolled. Table 1 shows the characteristics of each enrolled study. All studies contained at least one treatment arm using PEG-IFN and RBV for chronic hepatitis C. There were 16797 male and 10254

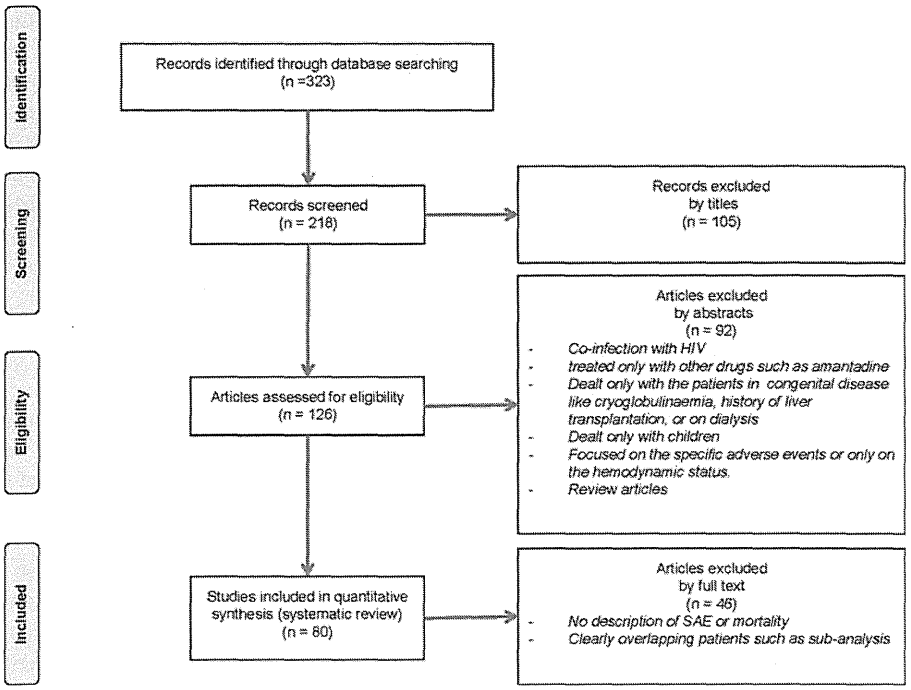

Fig. 1 The literature-search and study-selection process. *SAE* serious adverse events

females and the sex was not reported in the remaining 518 patients. The mean age was 45.9 years. A total of 14401 patients were treated with PEG-IFN alpha-2a/RBV, and 13168 with PEG-IFN alpha-2b/RBV. PEG-IFN alpha-2a was used at a fixed dose of 180–360 μg/body/week, and PEG-IFN alpha-2b at weight-based doses of 0.35–3.0 μg/kg/week. The RBV dose was fixed in 36 treatment arms and weight-based in 117 treatment arms. Treatment duration ranged from 12 to 72 weeks. The numbers of patients with HCV genotypes 1, 2, 3, and 4–6 were 18082, 3427, 3519, and 842, respectively. The genotype was not reported in the remaining 1699 patients. The treatment protocol is described in Supplementary Table 1.

Primary outcome

A total of 50 deaths from all causes were observed in the enrolled studies. Of these, sixteen were considered by the authors to be treatment-related. The crude overall and treatment-related mortality rates were 0.18 % (95 % CI 0.13–0.24 %) and 0.058 % (0.033–0.094 %), respectively. There was no evidence of heterogeneity among studies for mortality and treatment-related mortality ($I^2 = 0$ in both). The causes of mortality were suicide ($N = 6$), drug intoxication ($N = 6$), myocardial infarction ($N = 3$), sepsis ($N = 3$), aortic dissection ($N = 2$), traffic accident ($N = 2$), HCC ($N = 2$), rupture of a cerebral aneurysm ($N = 1$), bronchitis ($N = 1$), syncope ($N = 1$), pulmonary tuberculosis ($N = 1$), and unknown causes ($N = 22$). The six cases of suicide, the three of sepsis, two of drug intoxication, two of myocardial infarction, one of HCC, one of syncope, and one of pulmonary tuberculosis were considered by the investigators to be treatment-related mortality.

Subgroup analysis did not reveal any difference in mortality according to type and dose of PEG-IFN or in relation to duration of treatment (Fig. 2).

Secondary outcome

Seventy-two studies with 135 treatment arms including 23996 patients reported SAEs. They reported SAEs such as anemia requiring transfusion, neutropenia below 500/mm^3, hypothyroidism, psychosis, pneumonia, and cellulitis. SAEs were not discriminated from other adverse events in the remaining eighteen studies. The crude SAE rate was 7.08 % (95 % CI 6.75–7.41 %). Significant heterogeneity among studies was found for this outcome ($I^2 = 94.1$ %). SAE rates were higher in PEG-IFN alpha-2a than in PEG-IFN alpha-2b (7.45 vs. 6.74 %). In a subgroup analysis of the type and dose of PEG-IFN and duration of treatment, higher SAE rates were observed for intensive (270–360 μg) than for standard (180 μg) doses and for extended (>48 weeks) than for standard (48 weeks) treatment duration in patients treated with PEG-IFN alpha-2a, and for standard (1.5 μg/kg) than for lower (≤1.0 μg/kg) doses in patients treated with PEG-IFN alpha-2b (Fig. 3). However, heterogeneity remained evident in all subgroups.

Table 1 Characteristics of the enrolled studies

Study	Peginterferon type and dose	Ribavirin	Duration, weeks[a]	Patients, *N*	Male, *N*	Age, years (mean)	BW, kg (mean)	Ethnic group, *N*				HCV genotype, *N*			
								Caucasian	African	Asian	Other	G1	G2	G3	G4–6
Abergel [26]	2b 0.75 μg/kg	800 mg, fixed	48	102	70	51.1	NR	NR	NR	NR	NR	54	9	28	11
	2b 1.5 μg/kg	800 mg, fixed	48	101	65	49.3	NR	NR	NR	NR	NR	50	11	30	10
Alfaleh [27]	2b 100 μg	800 mg, fixed	48	48	22	48.4	NR	0	0	0	48	10	NR	NR	28
Andriulli [28]	2a 180 μg	1000–1200 mg	12[a]	61	30	52.5	70.6	NR	NR	NR	NR	0	52	9	0
	2a 180 μg	1000–1200 mg	12[a]	59	35	52.7	73	NR	NR	NR	NR	0	50	9	0
	2a 180 μg	1000–1200 mg	24[a]	24	18	47	71	NR	NR	NR	NR	0	10	14	0
Angelico [29]	2a 180 μg	800 mg, fixed	48[a]	42	NR	NR	NR	NR	NR	NR	NR	NR	NR	NR	NR
	2a 180 μg	800 mg, fixed	48[a]	57	NR	NR	NR	NR	NR	NR	NR	NR	NR	NR	NR
Ascione [14]	2b 1.5 μg/kg	1000–1200 mg	24–48[a]	160	94	48.9	69.9	160	0	0	0	92	50	17	1
	2a 180 μg	1000–1200 mg	24–48[a]	160	81	51.3	70.4	160	0	0	0	89	49	18	4
Benhamou [30]	2b 1.5 μg/kg	1000–1200 mg	24–48[a]	325	210	45.1	NR	271	12	14	28	226	NR	NR	10
Berg [31]	2a 180 μg	800 mg, fixed	48	12	5	44	70	11	0	1	0	10	0	2	0
	2a 180 μg	1000–1200 mg	48	52	46	44	83	47	2	3	0	35	6	6	5
Berg [32]	2a 180 μg	800 mg, fixed	48	230	128	42.7	76.3	222	2	6	0	230	0	0	0
	2a 180 μg	800 mg, fixed	72	225	122	42.7	75.3	213	3	6	3	225	0	0	0
Berg [33]	2b 1.5 μg/kg	800–1400 mg	48	225	128	42.8	NR	NR	NR	NR	NR	225	0	0	0
Bosques-Padilla [34]	2a 180 μg	1000–1200 mg	48	14	8	46	75	0	0	0	14	11	NR	NR	NR
Brady [35]	2b 1.5 μg/kg	800–1400 mg	48	311	156	45[b]	84.8	225	37	13	36	308	0	0	3
	2b 3.0 μg/kg	800–1400 mg	48[a]	299	149	45[b]	84.5	203	37	19	40	295	0	0	4
Brandao [36]	2a 180 μg	800 mg, fixed	48	31	19	40.8	76.4	26	0	2	3	31	0	0	0
	2a 180 μg	800 mg, fixed	24	54	46	42.3	80.7	50	2	0	2	0	NR	NR	NR
	2a 180 μg	800 mg, fixed	24	32	19	41.1	73.8	26	0	NR	6	32	0	0	0
Bressler [37]	2a 180 μg	1000–1200 mg	48	20	12	47.3	99	NR	NR	NR	NR	14	NR	NR	NR
	2a 270 μg	1000–1200 mg	48	20	14	44.3	98	NR	NR	NR	NR	14	NR	NR	NR
Bronowicki [38]	2a 180 μg	800 mg, fixed	24	516	306	46.2	70.8	NR	NR	NR	NR	NR	NR	NR	NR
Bruno [5]	2b 100 μg	1000–1200 mg	48[a]	163	101	49.9	69.4	NR	NR	NR	NR	163	0	0	0
Carr [39]	2b 1.5 μg/kg	1000–1200 mg	48	206	147	48	NR	160	26	4	16	166	NR	NR	NR
Ciancio [40]	2a 180 μg	1000–1200 mg	48	81	60	50	NR	NR	NR	NR	NR	66	9	3	3
Dalgard [41]	2b 1.5 μg/kg	800–1400 mg	24	150	97	38[b]	77	NR	NR	NR	NR	0	31	119	0
	2b 1.5 μg/kg	800–1400 mg	14	148	95	38[b]	79	NR	NR	NR	NR	0	29	119	0
Diago [42]	2a 180 μg	1000–1200 mg	48	28	21	40[b]	75.8	NR	NR	NR	NR	28	0	0	0
	2a 270 μg	1000–1200 mg	48[a]	20	15	44.5[b]	74.1	NR	NR	NR	NR	20	0	0	0
	2a 360 μg	1000–1200 mg	48[a]	24	20	41[b]	79	NR	NR	NR	NR	24	0	0	0

Table 1 continued

Study	Peginterferon type and dose	Ribavirin	Duration, weeks[a]	Patients, *N*	Male, *N*	Age, years (mean)	BW, kg (mean)	Ethnic group, *N*				HCV genotype, *N*			
								Caucasian	African	Asian	Other	G1	G2	G3	G4–6
Ferenci [43]	2a 180 μg	1000–1200 mg	48	95	65	44	NR	NR	NR	NR	NR	95	0	0	0
Ferenci [44]	2a 180 μg	400 mg, fixed	24	141	87	36.2	73.1	NR	NR	NR	NR	0	19	122	0
	2a 180 μg	800 mg, fixed	24	141	84	36.8	71.1	NR	NR	NR	NR	0	18	123	0
Ferenci [45]	2a 180 μg	1000–1200 mg	72[a]	150	98	44.3	76.9	NR	NR	NR	NR	134	0	0	16
	2a 180 μg	1000–1200 mg	48	139	90	45.1	78.5	NR	NR	NR	NR	127	0	0	12
Fried [4]	2a 180 μg	1000–1200 mg	48	453	324	42.8	79.8	372	27	28	26	298	54	86	13
Fried [46]	2a 180 μg	1200 mg, fixed	48	46	37	47.1	98.4	32	4	NR	10	46	0	0	0
	2a 180 μg	1600 mg, fixed	48	47	41	49.6	100.3	29	6	NR	12	47	0	0	0
	2a 270 μg	1200 mg, fixed	48	47	35	47.1	101	35	4	NR	8	47	0	0	0
	2a 270 μg	1600 mg, fixed	48	47	37	48.5	97	32	5	NR	10	47	0	0	0
Gish [47]	2a 180 μg	1000–1200 mg	24–48[a]	45	32	49	80	38	NR	NR	NR	NR	NR	NR	NR
Glue [48]	2b 0.35 μg/kg	600–800 mg	24	12	NR	39.8	65.6	NR	NR	NR	NR	9	NR	NR	NR
	2b 0.7 μg/kg	600–1200 mg	24	18	NR	39.8	65.6	NR	NR	NR	NR	5	NR	NR	NR
	2b 1.4 μg/kg	600–1200 mg	24	18	NR	39.8	65.6	NR	NR	NR	NR	4	NR	NR	NR
Hadziyannis [6]	2a 180 μg	1000–1200 mg	24	280	185	42	77.1	254	9	16	1	118	53	91	NR
	2a 180 μg	1000–1200 mg	48	436	287	43	77.3	394	11	26	5	271	66	87	NR
	2a 180 μg	800 mg, fixed	48	361	226	42.6	77	315	11	31	4	250	46	53	NR
	2a 180 μg	800 mg, fixed	24	207	140	41.2	78.3	183	7	14	3	101	39	57	NR
Hasan [49]	2b 1.5 μg/kg	1000–1200 mg	48	21	16	NR	NR	0	19	2	0	4	0	0	17
Helbling [50]	2a 180 μg	600–800 mg	48	60	36	47[b]	73	NR	NR	NR	NR	25	7	24	3
	2a 180 μg	1000–1200 mg	48	64	45	47[b]	74	NR	NR	NR	NR	30	11	18	4
Herrine [51]	2a 180 μg	800–1000 mg	48	32	24	48	NR	NR	NR	NR	NR	25	NR	NR	NR
Hezode [52]	2a 180 μg	1000–1200 mg	48	82	46	45[b]	NR	76	2	4	0	82	0	0	0
Ide [53]	2b 1.5 μg/kg	600–1000 mg	48	56	26	55.3	NR	0	0	56	0	56	0	0	0
	2b 1.5 μg/kg	600–1000 mg	48–68[a]	57	30	54.6	NR	0	0	57	0	57	0	0	0
Jacobson [54]	2b 1.0 μg/kg	1000–1200 mg	48	161	122	49.2	NR	118	23	NR	20	145	NR	NR	NR
	2b 1.5 μg/kg	800 mg, fixed	48	160	117	49.8	NR	106	27	NR	27	141	NR	NR	NR
Jacobson [55]	2b 1.5 μg/kg	800 mg, fixed	24–48[a]	2444	1560	45.8	83.8	1926	237	59	222	1506	526	386	23
	2b 1.5 μg/kg	800–1400 mg	24–48[a]	2469	1539	45.8	84	1993	208	59	209	1512	499	421	33
Jensen [56]	2a 180 μg	1000–1200 mg	48	313	212	48.5	80.9	282	25	NR	6	284	1	8	19
	2a 180 μg	1000–1200 mg	72	156	107	49.4	81.2	137	17	NR	2	142	1	5	8
	2a 360 μg	1000–1200 mg	48[a]	156	94	48.8	81.1	141	10	NR	5	142	3	4	5
	2a 360 μg	1000–1200 mg	72[a]	317	203	48.1	81.5	279	29	NR	9	288	2	7	19

Table 1 continued

Study	Peginterferon type and dose	Ribavirin	Duration, weeks[a]	Patients, *N*	Male, *N*	Age, years (mean)	BW, kg (mean)	Ethnic group, *N*				HCV genotype, *N*			
								Caucasian	African	Asian	Other	G1	G2	G3	G4–6
Kamal [57]	2b 1.5 μg/kg	1000–1200 mg	24	95	49	41.6	NR	NR	NR	NR	NR	0	0	0	95
	2b 1.5 μg/kg	1000–1200 mg	36	96	51	43.9	NR	NR	NR	NR	NR	0	0	0	96
	2b 1.5 μg/kg	1000–1200 mg	48	96	50	41.2	NR	NR	NR	NR	NR	0	0	0	96
Kamal [58]	2b 1.5 μg/kg	10.6 mg/kg	24[a]	69	37	41[b]	NR	NR	NR	NR	NR	69	0	0	0
	2b 1.5 μg/kg	10.6 mg/kg	36[a]	79	32	40.5[b]	NR	NR	NR	NR	NR	79	0	0	0
	2b 1.5 μg/kg	10.6 mg/kg	48[a]	160	100	42.2	NR	NR	NR	NR	NR	160	0	0	0
	2b 1.5 μg/kg	10.6 mg/kg	48	50	26	43.2	NR	NR	NR	NR	NR	50	0	0	0
Kawaoka [59]	2b 1.0 μg/kg	600–1000 mg	24	26	9	57[b]	53	0	0	26	0	0	26	0	0
	2b 1.5 μg/kg	600–1000 mg	24	27	15	55[b]	61	0	0	27	0	0	27	0	0
Khattab [60]	2b 1.5 μg/kg	800–1400 mg	48	49	34	37	NR	0	49	0	0	0	0	0	49
Kuboki [61]	2a 180 μg	600–1000 mg	48	100	74	52[b]	66.7	0	0	100	0	85	15	0	0
	2a 180 μg	600–1000 mg	48	99	62	52	62.8	0	0	99	0	99	0	0	0
Lagging [62]	2a 180 μg	800 mg, fixed	12	194	123	41.5	79.8	NR	NR	NR	NR	0	55	137	0
	2a 180 μg	800 mg, fixed	24	188	105	42	76.5	NR	NR	NR	NR	0	49	139	0
Langlet [63]	2a 180 μg	1000–1200 mg	24–48[a]	314	173	45.4	73.1	278	24	7	5	166	NR	NR	49
Lee [64]	2b 1.5 μg/kg	1000–1200 mg	24	76	53	44.6	67.8	0	0	76	0	38	38	0	0
Liu [65]	2a 180 μg	1000–1200 mg	24	154	88	54	67.6	0	0	154	0	154	0	0	0
	2a 180 μg	1000–1200 mg	48	154	87	53	65.8	0	0	154	0	154	0	0	0
Lodato [66]	2b 1.0–1.5 μg/kg	10.6 mg/kg	24–48[a]	43	23	49.6	NR	NR	NR	NR	NR	NR	NR	NR	NR
	2b 1.5 μg/kg	10.6 mg/kg	24–48[a]	22	12	48.7	NR	NR	NR	NR	NR	NR	NR	NR	NR
Mangia [7]	2b 1.0 μg/kg	1000–1200 mg	12	133	NR	NR	NR	NR	NR	NR	NR	0	102	31	0
	2b 1.0 μg/kg	1000–1200 mg	24	80	NR	NR	NR	NR	NR	NR	NR	0	58	22	0
	2b 1.0 μg/kg	1000–1200 mg	24	70	39	49.7	69.5	NR	NR	NR	NR	0	53	17	0
Manns [3]	2b 1.5 μg/kg	1000–1200 mg	48[a]	514	346	44	83	NR	NR	NR	NR	349	NR	NR	12
	2b 1.5 μg/kg	800 mg, fixed	48	511	321	43	82	NR	NR	NR	NR	348	NR	NR	16
Marcellin [67]	2b 1.5 μg/kg	800–1200 mg	24[a]	10	8	51.4	75.8	10	0	0	0	10	0	0	0
Marcellin [68]	2a 180 μg	1000–1200 mg	24–48[a]	318	201	45.1	NR	256	17	11	34	212	47	47	NR
McHutchison [15]	2a 180 μg [15]	1000–1200 mg	48	1035	613	47.6	82.8	733	200	20	82	1035	0	0	0
	2b 1.0 μg/kg	800–1400 mg	48	1016	607	47.5	83.4	724	187	21	84	1016	0	0	0
	2b 1.5 μg/kg	800–1400 mg	48	1019	613	47.5	84	732	183	10	94	1019	0	0	0
McHutchison [69]	2a 180 μg	1000–1200 mg	48	114	76	50[b]	NR	100	10	2	2	114	0	0	0
Mecenate [70]	2a 180 μg	1000–1200 mg	12[a]	72	NR	42[b]	NR	NR	NR	NR	NR	0	NR	NR	0
	2a 180 μg	1000–1200 mg	24[a]	67	54	45[b]	NR	NR	NR	NR	NR	0	37	30	0
	2a 180 μg	1000–1200 mg	24[a]	71	NR	42[b]	NR	NR	NR	NR	NR	0	NR	NR	0